Image Reconstruction from Videos Distorted by Atmospheric Turbulence

Xiang Zhu and Peyman Milanfar

Electrical Engineering Department
University of California at Santa Cruz, CA, 95064
xzhu@soe.ucsc.edu

ABSTRACT

To correct geometric distortion and reduce blur in videos that suffer from atmospheric turbulence, a multi-frame image reconstruction approach is proposed in this paper. This approach contains two major steps. In the first step, a B-spline based non-rigid image registration algorithm is employed to register each observed frame with respect to a reference image. To improve the registration accuracy, a symmetry constraint is introduced, which penalizes inconsistency between the forward and backward deformation parameters during the estimation process. A fast Gauss-Newton implementation method is also developed to reduce the computational cost of the registration algorithm. In the second step, a high quality image is restored from the registered observed frames under a Bayesian reconstruction framework, where we use L_1 norm minimization and a bilateral total variation (BTV) regularization prior, to make the algorithm more robust to noise and estimation error. Experiments show that the proposed approach can effectively reduce the influence of atmospheric turbulence even for noisy videos with relatively long exposure time.

Keywords: Image reconstruction, atmospheric turbulence, non-rigid image registration, bilateral total variation (BTV).

1. INTRODUCTION

Atmospheric turbulence caused by variation of refractive index along the optical transmission path can strongly affect the performance of long-distance imaging systems.[1,2] It produces geometric distortion, motion blur (if the exposure time is not sufficiently short), and sometimes out-of-focus blur when the turbulence is violent. The imaging process can be modeled as:

$$\mathbf{g}_k = \mathbf{B}_k\mathbf{F}_k\mathbf{z} + \varepsilon \tag{1}$$

where $\mathbf{z}$ denotes the ideal image without turbulence distortion or blur, $\mathbf{F}_k$ and $\mathbf{B}_k$ represent the deformation matrix and the blurring matrix respectively, ε denotes additive noise, and $\mathbf{g}_k$ is the k-th observed frame.

Several approaches have been proposed to solve this problem,[3–5] and since the information in a single frame is usually insufficient to recover, all these works are based on videos or image sequences under the assumption that the scene is static. For example, in the article[5] an experiment is provided to illustrate that the local turbulent motion has a zero-mean Gaussian distribution, and thus the geometric distortion can be removed by simply averaging the observed frames. Such averaged image, though even more blurred than the original data, can serve as a reference frame to register each observed frame.

Current restoration algorithms for atmospheric imaging systems can generally be divided into two main categories. One important category is based on multi-frame reconstruction. This type of approach first requires a non-rigid image registration technique to register each observed frame and use the registration parameters to further estimate the deformation matrix $\mathbf{F}_k$. Then, a sharp image is reconstructed under a Bayesian image reconstruction framework. In the article[5] Shimizu and Okutomi proposed an improved B-spline based non-rigid registration method for the turbulence distortion estimation. They introduced a stabilization term into the cost function, and claimed that this term enables more accurate estimation in the regions containing less texture. A Gauss-Newton method was employed to optimize their cost function. However, direct implementation of the algorithmic procedure of the registration method described in[5] is time consuming. Besides, the Bayesian

reconstruction method proposed in,[5] which uses L_2 norm and Tikhonov regularization term, is also sensitive to the assumed model of noise and the registration error.

Another class of approaches employs image selection and fusion methods to reduce the blurring effects caused by turbulence.[4] The frame selection technique finds out frames of the best quality (lucky frame) from a short-exposure video stream, and the output image is produced by fusing these lucky frames.[6,7] The problem of this approach is the very low probability of existence of a whole high-quality frame. To alleviate this problem Vorontsov introduced the idea of "lucky region",[8–10] where it is shown that for short-exposure images turbulence creates "mutations" in local image quality, and randomly makes some regions sharper, which are called lucky regions. The lucky regions can be detected by a sharpness metric, and then fused to produce a high quality image.[8–10] A difficulty with this method is again the low probability of the appearance of lucky regions. Although high-quality regions happen more frequently than high-quality frames, this method generally requires a large number (usually hundreds) of frames to create one single sharp image. Another problem is that this method is applicable only for short-exposure videos, while for long-exposure videos motion blur makes the lucky regions too rare to be useful.

In this paper, we propose a new multi-frame reconstruction method to restore a single image from videos influenced by atmospheric turbulence. This method includes a high-performance non-rigid registration technique and a Bayesian reconstruction algorithm that is robust to noise and estimation error. Compared with the lucky region selection and fusion method, our approach requires fewer frames, and is applicable for videos with longer exposure time.

2. PROPOSED APPROACH

This approach consists of two major stages: image registration and multi-frame reconstruction. In the registration part, we introduce a symmetry constraint, which can further improve the registration accuracy. A fast implementation was also developed so that the calculation cost can be significantly reduced. In the reconstruction part, we use L_1 norm and bilateral total variation (BTV) regularization term to enhance image quality.

2.1 Non-rigid Image Registration

Assume G (also denoted as $\mathbf{g}$ in vector form) represents an observed distorted image, and R denotes a reference image without turbulent deformation (which can be obtained by averaging the frame sequence). A non-rigid deformation model can be employed to describe the geometric distortion between these two images. In this model, the complex motion is represented by the movement of n control points, whose initial positions $\hat{\mathbf{x}}_{0i} = (\hat{x}_{0i}, \hat{y}_{0i})^T$ $(i = 1, \cdots, n)$ are equally spaced on the given image G. The displacement of all the control points on the reference image R is denoted as the deformation vector: $\overrightarrow{\mathbf{p}} = [\Delta\hat{x}_1, \ldots, \Delta\hat{x}_n, \Delta\hat{y}_1, \ldots, \Delta\hat{y}_n]^T$, where $\Delta\hat{x}$ and $\Delta\hat{y}$ (also called deformation parameters) are the horizontal and vertical displacement from the initial position.[5,11] The deformed position of any given pixel located at $\mathbf{x} = (x, y)^T$ from image G can then be described as:

$$\mathbf{W}(\mathbf{x}; \overrightarrow{\mathbf{p}}) = \mathbf{x} + \mathbf{A}(\mathbf{x})\overrightarrow{\mathbf{p}}, \tag{2}$$

where $\mathbf{A}(\mathbf{x})$ denotes the basis function matrix for $\mathbf{x}$:

$$\mathbf{A}(\mathbf{x}) = \begin{bmatrix} c_1 & \ldots & c_n & 0 & \ldots & 0 \\ 0 & \ldots & 0 & c_1 & \ldots & c_n \end{bmatrix}, \tag{3}$$

and $\mathbf{A}(\mathbf{x})\overrightarrow{\mathbf{p}}$ is the motion vector, which is a linear combination of the movements of all control points. The weight, or say spline basis c_i is determined by the distance between $\mathbf{x}$ and $\hat{\mathbf{x}}_{0i}$ using B-spline interpolation:

$$c_i = \beta\left(\frac{x - \hat{x}_{0i}}{h_x}\right)\beta\left(\frac{y - \hat{y}_{0i}}{h_y}\right). \tag{4}$$

$$\beta(t) = \begin{cases} 2/3 - (1 - |t|/2)t^2 & \text{, if } 0 \le |t| \le 1 \\ (2 - |t|)^3/6 & \text{, if } 1 < |t| < 2 \\ 0 & \text{, otherwise} \end{cases} \tag{5}$$

where h_x and h_y are the horizontal and vertical intervals between neighboring control points.

In the classic B-spline based registration approach, the deformation vector can be estimated by minimizing the following cost function:[11]

$$C(\overrightarrow{\mathbf{p}}) = \sum_{\mathbf{x}} |R(\mathbf{W}(\mathbf{x}; \overrightarrow{\mathbf{p}})) - G(\mathbf{x})|^2 \tag{6}$$

However, because the above function lacks prior constraint, the resulting estimate is unstable and gets easily stuck in local minima. To improve this method, a stabilization constraint is proposed in article[5] , which makes the estimated deformation parameters remain small in the regions that have less texture (low image gradient). However, we know that the deformation caused by atmospheric turbulence is independent from image content. In other words, such stabilization constraint would bring unnecessary bias into the estimation.

To accurately estimate the deformation vector and further the motion vectors from image R to G, we instead introduce a symmetry constraint[12,13] into the B-spline registration algorithm. This constraint is based on an important property that the registration should be symmetric or inverse consistent.[12] Let $\overrightarrow{\mathbf{p}}$ denote the deformation vector that can transform R into G (forward deformation), and $\overleftarrow{\mathbf{p}}$ denote the inverse vector that transform G into R (backward deformation). Then approximately we have: $\overrightarrow{\mathbf{p}} = -\overleftarrow{\mathbf{p}}$. Combing the two sets of vectors into one vector: $\mathbf{p}^T = [\overrightarrow{\mathbf{p}}^T, \overleftarrow{\mathbf{p}}^T]$, the proposed cost function to minimize becomes:

$$C(\mathbf{p}) = \sum_{\mathbf{x}} |R(\mathbf{W}(\mathbf{x}; \overrightarrow{\mathbf{p}})) - G(\mathbf{x})|^2 + \sum_{\mathbf{x}} |G(\mathbf{W}(\mathbf{x}; \overleftarrow{\mathbf{p}})) - R(\mathbf{x})|^2 + \gamma(\overrightarrow{\mathbf{p}} + \overleftarrow{\mathbf{p}})^T(\overrightarrow{\mathbf{p}} + \overleftarrow{\mathbf{p}}) \tag{7}$$

where scalar γ controls the effect of symmetry constraint.

Gauss-Newton method is used to optimize the above $C(\mathbf{p})$, and the update of the parameter set $\mathbf{p}$ can be derived as follows:

$$\mathbf{p}^{l+1} = \mathbf{p}^l - \mathbf{H}^{-1}\mathbf{b} \tag{8}$$

$$\mathbf{H} = \begin{bmatrix} \overrightarrow{\mathbf{H}} + \gamma\mathbf{I} & \gamma\mathbf{I} \\ \gamma\mathbf{I} & \overleftarrow{\mathbf{H}} + \gamma\mathbf{I} \end{bmatrix}, \quad \mathbf{b}^T = \left[(\overrightarrow{\mathbf{b}} + \overrightarrow{\mathbf{p}}^l + \overleftarrow{\mathbf{p}}^l)^T, (\overleftarrow{\mathbf{b}} + \overrightarrow{\mathbf{p}}^l + \overleftarrow{\mathbf{p}}^l)^T\right] \tag{9}$$

$$\overrightarrow{\mathbf{H}} = \textstyle\sum_{\mathbf{x}} \overrightarrow{\mathbf{d}}(\mathbf{x})\overrightarrow{\mathbf{d}}(\mathbf{x})^T, \quad \overleftarrow{\mathbf{H}} = \textstyle\sum_{\mathbf{x}} \overleftarrow{\mathbf{d}}(\mathbf{x})\overleftarrow{\mathbf{d}}(\mathbf{x})^T \tag{10}$$

$$\overrightarrow{\mathbf{b}} = \textstyle\sum_{\mathbf{x}} \overrightarrow{\mathbf{d}}(\mathbf{x})[R(\mathbf{W}(\mathbf{x}; \overrightarrow{\mathbf{p}}^l)) - G(\mathbf{x})], \quad \overleftarrow{\mathbf{b}} = \textstyle\sum_{\mathbf{x}} \overleftarrow{\mathbf{d}}(\mathbf{x})[G(\mathbf{W}(\mathbf{x}; \overleftarrow{\mathbf{p}}^l)) - R(\mathbf{x})] \tag{11}$$

$$\overrightarrow{\mathbf{d}}(\mathbf{x})^T = \frac{\partial R(\mathbf{W}(\mathbf{x}; \overrightarrow{\mathbf{p}}^l))}{\partial \mathbf{W}}\mathbf{A}(\mathbf{x}), \quad \overleftarrow{\mathbf{d}}(\mathbf{x})^T = \frac{\partial G(\mathbf{W}(\mathbf{x}; \overleftarrow{\mathbf{p}}^l))}{\partial \mathbf{W}}\mathbf{A}(\mathbf{x}) \tag{12}$$

In the above process, the computational cost for calculating the matrices $\overrightarrow{\mathbf{H}}$ and $\overleftarrow{\mathbf{H}}$ is tremendous if it is implemented directly. For instance, assuming that the size of both R and G is 320×240, and the intervals $h_x = h_y = 16$, we have around 300 control points, and the size of $\overrightarrow{\mathbf{p}}$ would be 600×1. In Eq.(10) the matrix product $\overrightarrow{\mathbf{d}}(\mathbf{x})\overrightarrow{\mathbf{d}}(\mathbf{x})^T$ would cost at least $360,000$ multiplication operations, and this process needs to be repeated for all the 320×240 pixels in the image. Furthermore, if the size of the image increases with the intervals fixed, the corresponding number of the control points will increase, which means the computational complexity in calculating $\overrightarrow{\mathbf{d}}(\mathbf{x})\overrightarrow{\mathbf{d}}(\mathbf{x})^T$ for each pixel will also be raised.

To solve this problem, we use a fast implementation method for calculating $\overrightarrow{\mathbf{H}}$ and $\overleftarrow{\mathbf{H}}$. Take $\overrightarrow{\mathbf{H}}$ for instance. The gradient of image R at position $\mathbf{W}(\mathbf{x}; \overrightarrow{\mathbf{p}})$ can be denoted as:

$$\frac{\partial R(\mathbf{W}(\mathbf{x}; \overrightarrow{\mathbf{p}}))}{\partial \mathbf{W}} = [r_x(\mathbf{W}), r_y(\mathbf{W})] \tag{13}$$

We define B-spline basis vector $\mathbf{c_x} = [c_1, \ldots, c_n]^T$, and matrix $\mathbf{C_x} = \mathbf{c_x}\mathbf{c_x}^T$. Then $\overrightarrow{\mathbf{H}}$ can be computed through the following form:

$$\overrightarrow{\mathbf{H}} = \sum_{\mathbf{x}} \overrightarrow{\mathbf{H}}_{\mathbf{x}} \tag{14}$$

where:

$$\overrightarrow{\mathbf{H}}_{\mathbf{x}} = \begin{bmatrix} r_x(\mathbf{W})^2\mathbf{C_x} & r_x(\mathbf{W})r_y(\mathbf{W})\mathbf{C_x} \\ r_x(\mathbf{W})r_y(\mathbf{W})\mathbf{C_x} & r_y(\mathbf{W})^2\mathbf{C_x} \end{bmatrix} \tag{15}$$

In the Eq.(5), it can be observed that $\beta(t) = 0$ if $|t| \geq 2$, which means the value of each pixel can only influence the neighboring 4×4 control points in the update procedure. So, for the pixel at position $\mathbf{x}$, the basis vector $\mathbf{c_x}$ contains at most 16 non-zero entries. In other words, $\mathbf{C_x}$ is a sparse matrix with 256 non-zero entries, and among them, there are only 136 unique values, due to the symmetry of $\mathbf{C_x}$.

Hence we can see that each $\overrightarrow{\mathbf{H}}_\mathbf{x}$ contains 1024 non-zero entries, and requires 680 multiplications (136 for calculating $\mathbf{C_x}$, and 544 for calculating $\overrightarrow{\mathbf{H}}_\mathbf{x}$ through Eq.(15)). This number is independent from either the number of control points or the size of the images. Implementation based on this derivation can drastically reduce the computational cost for the non-rigid registration procedure. For example, on Intel Core 2 CPU (3.00 GHz) the execution time for registering 320×240 images using MATLAB is around 2 hours for direct implementation of the iteration process (8)-(12), but it only requires 10 minutes for the above new method,

2.2 Bayesian Image Reconstruction

The Bayesian reconstruction models the imaging process described in Eq.(1), and the output image is estimated by minimizing a cost function that can generally be defined as:

$$J(\mathbf{z}) = \sum_k \parallel \mathbf{g}_k - \mathbf{B}_k\mathbf{F}_k\mathbf{z} \parallel_p^p + \lambda R(\mathbf{z}) \tag{16}$$

where the data fitting term uses L_p norm ($1 \leq p \leq 2$), and $R(\cdot)$ represents a regularization term, which can help the algorithm to remove noise from the final result and improve the rate of convergence. The effect of this term can be adjusted by tuning the scalar λ.

For many Bayesian estimation algorithms, the additive noise is assumed to be white and Gaussian, and thus the least-squares estimator (L_2 norm) is favored. However, in practice the real noise may not be Gaussian. Meanwhile, the error caused by the image registration stage should also be taken into account. In article[14] it is illustrated that the least-square estimation from a set of data contaminated by non-Gaussian outliers may produce an image with visually apparent errors, while L_1 norm results in pixelwise median of all the measurements, and thus makes the estimator more robust to real noise and registration error. To further suppress random noise and protect high frequency image content (such as edge pixels), BTV regularization term is employed:[14]

$$R_{BTV}(\mathbf{z}) = \underbrace{\sum_{l=-P}^{P} \sum_{m=0}^{P}}_{l+m\geq 0} \alpha^{|m|+|l|} \parallel \mathbf{z} - \mathbf{S}_x^l\mathbf{S}_y^m\mathbf{z} \parallel_1 \tag{17}$$

Here $0 < \alpha < 1$ gives a spatially decaying effect to the summation of the regularization term. Matrices $\mathbf{S}_x^l$ and $\mathbf{S}_y^m$ shift the image $\mathbf{z}$ by l and m pixels in horizontal and vertical directions respectively.[14]

The cost function for the Bayesian reconstruction now becomes:

$$J(\mathbf{z}) = \sum_k \parallel \mathbf{g}_k - \mathbf{B}_k\mathbf{F}_k\mathbf{z} \parallel_1 + \lambda \underbrace{\sum_{l=-P}^{P} \sum_{m=0}^{P}}_{l+m\geq 0} \alpha^{|m|+|l|} \parallel \mathbf{z} - \mathbf{S}_x^l\mathbf{S}_y^m\mathbf{z} \parallel_1 \tag{18}$$

The only problem remained is that the temporally and spatially variant blurring matrices $\mathbf{B}_k$ are unknown and difficult to estimate. However, for long-term exposures the point-spread function (PSF) can be described reasonably by a Gaussian function:[15]

$$b(x, y) = Z \exp\left(-\frac{x^2 + y^2}{2\sigma_B^2}\right) \tag{19}$$

where the normalization factor Z makes the PSF satisfy:

$$\sum_{x,y} b(x, y) = 1, \tag{20}$$

and σ_B determines the spread of the blur kernel, whose value should be chosen according to the degree of blur of the observed video data. In practice, σ_B is tuned according the output image quality.[16,17]

(a) Original image (b) Deformed image (c) RMSE

Figure 1. Monte-Carlo simulation experiments testing the performance of different B-spline registration algorithms.

3. EXPERIMENTAL RESULTS

Monte-Carlo simulations are carried out to illustrate the performance of the proposed registration method. The test image (320×240) is given in Fig.1(a). (b) shows the image deformed by turbulence, which was simulated through the deformation model described in (2)-(5), where $h_x = h_y = 16$, and the deformation vectors $\overrightarrow{\mathbf{p}}_{true}$ were randomly generated. White Gaussian noise with standard deviation σ ranging from 0 to 7 was also added to the image pair. For each σ, 10 independent noise realizations were generated. After each registration test, the root mean squared error (RMSE) between the true motion vectors and the estimated motion vectors are calculated to indicate the algorithm's performance.

Three different algorithms were tested for comparison: the classic B-spline registration method without any prior constraint,[11] the stable B-spline registration method,[5] and the proposed method using symmetry constraint. For all these methods, the intervals were set to be the same: $h_x = h_y = 16$. The stabilization parameter for the stable registration method was set to be 5 as recommended in the article.[5] In our method, the symmetry constraint parameter $\gamma = 5,000$. For each σ, both mean and standard deviation of RMSE over the 10 different tests are calculated and shown in Fig.1(c). It can be observed that the proposed method offers a much more accurate estimation than the other two under all the noise strengths. It is also interesting to see that the stable B-spline registration method works worse than the classic one in this case, which is probably due to the fact, as we described in Section 2, that the stabilization term changes the value of deformation parameters according to the local image content, while the atmospheric turbulence is independent of the image content. The bias brought by the stabilization term may possibly reduce the estimation accuracy under some circumstances.

Finally, we give some real data reconstruction results using the proposed method and lucky region fusion method as comparison.[8–10] The first set of data shows the moon surface (400×400), where the scene is relatively clean, slightly blurred and with mild turbulence (see Fig.3(a)). Only 20 frames are taken for the reconstruction experiment, so that the amount of sharp regions (lucky region) is very limited. We can see that basically lucky region fusion method failed to recover high frequency content (Fig.3(b)), while the proposed method gives a significant improvement in image quality (Fig.3(c)).

The scene of the second video stream consists of a water tower located above the ground. The video is quite noisy and highly blurred (due to longer exposure time). 10 frames were taken from the video to produce the result image (300×220) demonstrated in Fig.3. Again, the lucky region method did not provide much improvement in the result, while the output of the proposed method looks sharper and clean, with some details fairly restored.

In these two set of experiments, the parameters for the non-rigid registration are the same as we used in the above Monte-Carlo simulations, and the parameters in the reconstruction part are set as: $\lambda = 0.2$, $\alpha = 0.6$, $P = 2$. The width of the PSF $\sigma_B = 2$ for the *Moon Surface* data, and $\sigma_B = 3$ for the *Water Tower* data.

4. CONCLUSIONS AND FUTURE WORK

We proposed a multi-frame image reconstruction approach to restore an image from a video sequence degraded by atmospheric turbulence. This approach consists of a B-spline based non-rigid image registration method

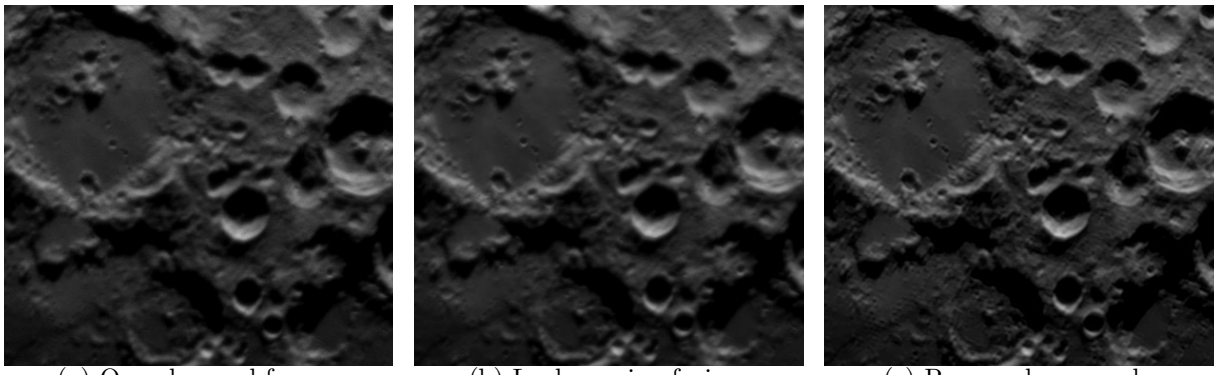

(a) One observed frame (b) Lucky region fusion (c) Proposed approach

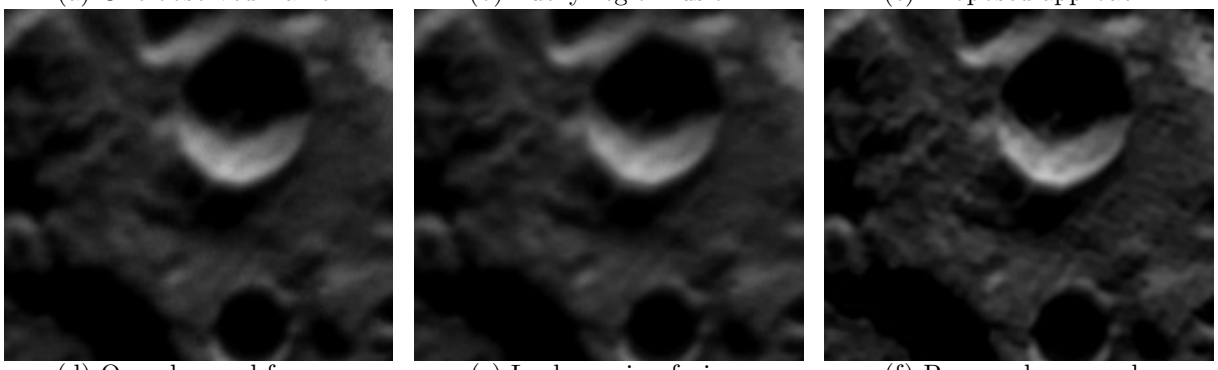

(d) One observed frame (e) Lucky region fusion (f) Proposed approach

Figure 2. Image reconstruction results using 20 frames taken from the video *Moon Surface* distorted by real atmospheric turbulence.

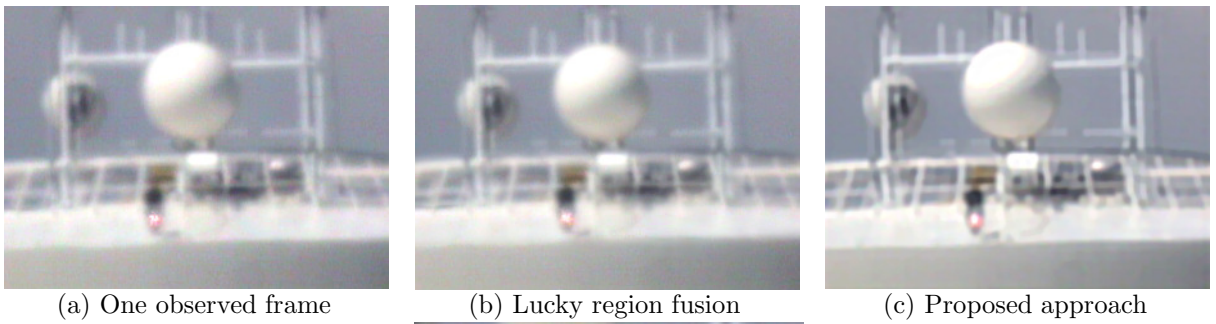

(a) One observed frame (b) Lucky region fusion (c) Proposed approach

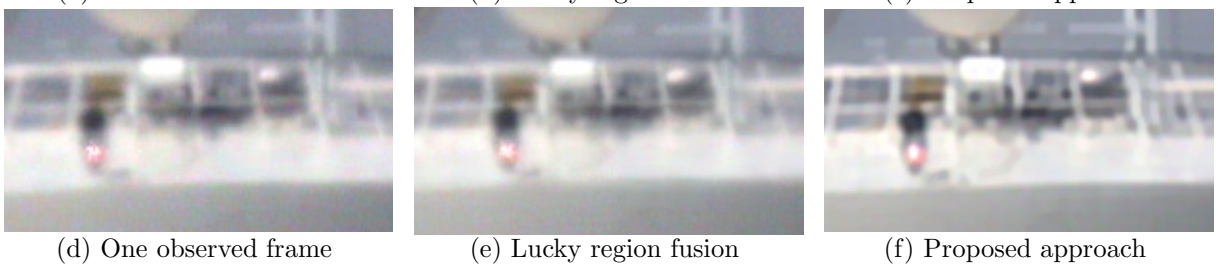

(d) One observed frame (e) Lucky region fusion (f) Proposed approach

Figure 3. Image reconstruction result using 10 frames taken from the video *Water Tower* distorted by real atmospheric turbulence.

followed by a Bayesian reconstruction algorithm. A symmetry constraint is introduced into the registration part and simulated experiments shows that this constraint efficiently improves the estimation accuracy. In the Bayesian reconstruction stage, L_1 norm minimization and BTV regularization prior are employed to make the algorithm more robust to noise and registration error. Real data experiments illustrate that the proposed approach can reduce the influence of atmospheric turbulence even for noisy videos with relatively long exposure time.

One disadvantage of the current reconstruction algorithm is that in the reconstruction stage it assumes the PSF to be time and space invariant, which is not the case in practice. For example, according to the study of lucky region, turbulence randomly makes some image regions sharper.[3,4] In our future work, local image sharpness metric and local PSF estimation algorithm will be investigated to see whether they can be implemented to improve the performance of the proposed approach, and to even make super-resolution reconstruction applicable for those highly distorted videos.

5. ACKNOWLEDGMENTS

The authors would like to thank Prof. Mikhail A. Vorontsov from the Intelligent Optics Lab of the University of Maryland for allowing us to use the video data *Water Tower*, and also thank Mr. Faisal A. Salem from University of Michigan and Dr. Joseph M. Zawodny from NASA Langley Research Center for providing us with the video *Moon Surface*.

REFERENCES

[1] Roggemann, M. C. and Welsh, B. M., "Imaging through turbulence," *CRC Press, Boca Raton, Fla.* (1996).

[2] Li, D., Mersereau, R. M., and Simske, S., "Atmospheric turbulence-degraded image restoration using principal components analysis," *IEEE Geoscience and Remote Sensing Letters* **4**, 340–344 (July 2007).

[3] Vorontsov, M. A., "Parallel image processing based on an evolution equation with anisotropic gain: integrated optoelectronic architectures," *J. Opt. Soc. Am. A* **16**, 1623–1637 (1999).

[4] Vorontsov, M. A. and Carhart, G. W., "Anisoplanatic imaging through turbulent media: image recovery by local information fusion from a set of short-exposure images," *J. Opt. Soc. Am. A* **18**, 1312–1324 (June 2001).

[5] Shimizu, M., Yoshimura, S., Tanaka, M., and Okutomi, M., "Super-resolution from image sequence under influence of hot-air optical turbulence," *CVPR 2008* , 1–8 (June 2008).

[6] Roggemann, M. C., Stoudt, C. A., and Welsh, B. M., "Image-spectrum signal-to-noise-ratio improvements by statistical frame selection for adaptive-optics imaging through atmospheric turbulence," *Optical Engineering* **33**, 3254–3264 (October 1994).

[7] Fried, D. L., "Probability of getting a lucky short-exposure image through turbulence," *Optical Society of America, Journal* **68**, 1651–1658 (1978).

[8] Aubailly, M., Vorontsov, M. A., Carhart, G. W., and Valley, M. T., "Image enhancement by local information fusion with pre-processing and composed metric," *Proceedings of SPIE* **7090** (2008).

[9] John, S. and Vorontsov, M. A., "Multiframe selective information fusion from robust error estimation theory," *IEEE Transactions on Image Processing* **14**, 577–584 (May 2005).

[10] Aubailly, M., Vorontsov, M. A., Carhat, G. W., and Valley, M. T., "Automated video enhancement from a stream of atmospherically-distorted images: the lucky-region fusion approach," *Proceedings of SPIE* **7463** (2009).

[11] Szeliski, R. and Coughlan, J., "Spline-based image registration," *International Journal of Computer Vision* **22**(93), 199–218 (1997).

[12] Farsiu, S., Elad, M., and Milanfar, P., "Constrained, globally optimal, multi-frame motion estimation," *IEEE/SP 13th Workshop on Statistical Signal Processing* , 1396–1401 (July 2005).

[13] Beg, M. F. and Khan, A., "Symmetric data attachment terms for large deformation image registration," *IEEE Transactions on Medical Imaging* **26**(9), 1179–1189 (2007).

[14] Farsiu, S., Robinson, M. D., Elad, M., and Milanfar, P., "Fast and robust multiframe super resolution," *IEEE Transactions on Image Processing* **13**, 1327–1344 (October 2004).

[15] Lagendijk, R. L. and Biemond, J., "Basis methods for image restoration and identification," *Handbook of Image and Video Processing, 2nd Edition* , 167–181 (2005).

[16] Zhu, X. and Milanfar, P., "A no-reference sharpness metric sensitive to blur and noise," *International Workshop on Quality of Multimedia Experience (QoMEX)* (2009).

[17] Zhu, X. and Milanfar, P., "Automatic parameter selection for denoising algorithms using a no-reference measure of image content," *Submitted to IEEE Trans. on Image Processing* .